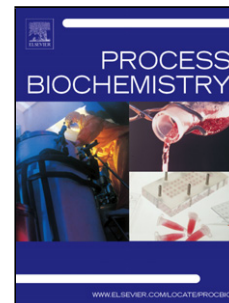


Journal Pre-proof

Inhibition of xanthine oxidase by theaflavin: possible mechanism for anti-hyperuricaemia effect in mice

Jianmin Chen (Conceptualization) (Methodology) (Writing - original draft), Qinglian Li (Software) (Investigation), Yaling Ye (Investigation) (Data curation), Mengnan Ran (Supervision) (Data curation), Zhipeng Ruan (Supervision) (Validation), Nan Jin (Writing - review and editing)



PII: S1359-5113(20)30145-8

DOI: <https://doi.org/10.1016/j.procbio.2020.06.024>

Reference: PRBI 12075

To appear in: *Process Biochemistry*

Received Date: 30 January 2020

Revised Date: 13 May 2020

Accepted Date: 25 June 2020

Please cite this article as: Chen J, Li Q, Ye Y, Ran M, Ruan Z, Jin N, Inhibition of xanthine oxidase by theaflavin: possible mechanism for anti-hyperuricaemia effect in mice, *Process Biochemistry* (2020), doi: <https://doi.org/10.1016/j.procbio.2020.06.024>

This is a PDF file of an article that has undergone enhancements after acceptance, such as the addition of a cover page and metadata, and formatting for readability, but it is not yet the definitive version of record. This version will undergo additional copyediting, typesetting and review before it is published in its final form, but we are providing this version to give early visibility of the article. Please note that, during the production process, errors may be discovered which could affect the content, and all legal disclaimers that apply to the journal pertain.

© 2020 Published by Elsevier.

Inhibition of xanthine oxidase by theaflavin: possible mechanism for anti-hyperuricaemia effect in mice

Jianmin Chen^{1,2*}, Qinglian Li¹, Yaling Ye¹, Mengnan Ran¹, Zhipeng Ruan^{1,2}, Nan Jin^{1,2}

1. School of Pharmacy and Medical technology, Putian University, Fujian, China

2. Key Laboratory of Pharmaceutical Analysis and Laboratory Medicine (Putian University), Fujian Province University, Fujian, China.

*Corresponding author:

School of Pharmacy and Medical technology, Putian University, 351100, Fujian, China

Tel: +86 0594 2787689; Fax: +86 0594 2787689

E-mail address: chenjianmin1985@sina.com ORCID: 0000-0003-2934-1493

Graphical abstract



Highlights

- Theaflavin reversibly inhibited xanthine oxidase activity in a competitive manner.
- Theaflavin quenched the fluorescence of the enzyme by forming complex with it.
- There was a single class of binding site on xanthine oxidase for Theaflavin.
- Theaflavin occupied the catalytic site of the enzyme to avoid entry of xanthine.
- Theaflavin presented uric acid reducing effect in hyperuricemic mice.

Abstract:

Xanthine oxidase (XO) catalyzes the oxidation of hypoxanthine to xanthine and then to uric acid. Excessive production of uric acid leads to hyperuricaemia. Due to the serious side effects of allopurinol, it is an urgent need to explore new XO inhibitors. Herein, the effects of theaflavin (TF1) on XO and anti-hyperuricaemia effect in hyperuricemic mice were investigated. Kinetic analysis indicate that TF1 is a reversible competitive inhibitor and has a significant inhibitory effect on XO with an IC_{50} value of $63.17 \pm 0.13 \mu\text{mol/L}$. Analysis of fluorescence spectra suggests that TF1 causes the obvious fluorescence quenching of XO, which is mainly driven by hydrophobic interactions and hydrogen bonds. Docking studies demonstrate that TF1 interacts with dozens of amino acid residues surrounded in the active cavity of XO, including Glu-879, Pro-1012, Thr-1010, Val-1011, Lys-771, Glu-802, Pro-1076, Leu-873, Leu-1014, Asn-768, Leu-648 and Phe-649. The inhibitory mechanism may be the insertion of TF1 into the active site of XO, which hinders the substrate xanthine to enter into the site. Furthermore, the results from animal experiments demonstrate that TF1 is effective in reducing serum uric acid in mice. These findings suggest that TF1 may be a potential drug candidate for the treatment of hyperuricaemia.

Key words: xanthine oxidase; theaflavin; inhibitory mechanism; molecular docking; anti-hyperuricaemia

1 Introduction

Xanthine oxidase (XO, EC 1.1.3.22), a member of xanthine oxidoreductase group, is found widely in mammalian tissues such as liver and intestine[1, 2]. It is a molecular mass 290 kD homodimer with each monomer containing two [2Fe-2S] centers, a flavin adenine dinucleotide cofactor and a molybdenum atom[3]. The molybdopterine center (Mo-pt) of each monomer acts independently during the process of catalysis, which catalyze the oxidation of xanthine to uric acid, superoxide anions and hydrogen peroxide in the presence of molecular oxygen[4]. The overproduction of uric acid in the serum will lead to hyperuricaemia, which increases the risk of the condition including gout, cardiovascular disease, chronic kidney disease and other metabolic disorders[5, 6]. Therefore, XO inhibitors may have the potential for the prevention or treatment of these diseases. Allopurinol is a commonly used drug for the treatment of hyperuricaemia and gout, but it may cause some serious side effects, including hepatitis, kidney disease, allergy and rash[7, 8]. Thus, the screening of new natural XO inhibitors should be further explored to provide more effective safe drugs to clinical application.

Flavonoids, various compounds found naturally in many fruits, vegetables, wine, chocolate and tea, have potential inhibitory effects on XO, and the recent progress in this field has been summarized [9]. Black tea made from the fresh leaves of *Camellia sinensis* via a fermentation process is the most popular tea in the world[10]. Theaflavins (TFs) are formed by the oxidation of flavanols (catechins and gallic catechins), a process called fermentation during the manufacture of tea, and have

great contribution to the color and flavor of black tea[11]. TFs consist of theaflavin and its galloyl esters: TF1, theaflavin-3-gallate, theaflavin-3'-gallate, and theaflavin-3,3'-digallate[11]. TFs have been reported to have various biological activities, such as antioxidant activity[12], antiviral activity[13], antiobesity activity[14], anticancer activity[15], anti-inflammatory effects[16], antidiabetic effects[17], and the bone loss in models of osteoporosis[18]. Although TFs have been reported to exhibit inhibitory effects on XO[19], the inhibitory types and mechanisms of TFs have not been investigated comprehensively so far. In addition, the effect of black tea aqueous extracts on hyperuricaemia has been reported recently[20], but whether the single component of the extracts may reduce the level of serum uric acid in hyperuricaemia animal model has still not been studied.

Therefore, in this work, we investigated the effects of theaflavin (TF1) on the activity of XO via using spectroscopy and molecular docking, as well as on the level of serum uric acid in hyperuricemic mice. We choose TF1 as the model drug, because it has the basic structure of TFs. The purpose of this study is to elucidate the inherent inhibitory mechanism of TF1 on the activity of XO, which may be helpful to design novel enzyme inhibitors with higher efficiency and better safety. In addition, the results of animal experiments will further provide fundamental data for TF1 in the treatment of hyperuricaemia and other related metabolic diseases.

2. Materials and methods

2.1 Materials

Theaflavin (>98%) was obtained from Kai-lai Biological Engineering Co., Ltd

(Xi'an, China). XO (35.7 units/mL, EC 1.17.3.2) derived from bovine milk was purchased from Sigma-Aldrich (St. Louis, MO, USA) without further purification. Xanthine, uric acid, phosphotungstic acid, lithium sulfate and potassium oxonate were bought from Aladdin Bio-Chem Technology Co.,LTD (Shanghai, China). All other chemicals used in this study were all analytical grade. During the whole research process, a Milli-Q-Plus ultra-pure water system of Millipore (Sartorius 611, Germany) was used to obtain the water needed in the experiments.

2.2 Inhibitory effects of TF1 on the activity of XO

The activity of XO was tested according to the method previously described with some modifications[21]. Briefly, 100 μ L of the test compound in DMSO and 200 μ L of XO (0.04 U/mL) in 0.2 mol/L PBS were mixed, and the mixture was stand for 5 min at room temperature. The control group was carried out by adding the equal volume solvent instead of compound itself. The reaction was started by pouring 2.7 mL of 0.1 mmol/L xanthine in PBS to the mixture. The OD (optical density) values of the mixtures were recorded at the wavelength of 290 nm per minute at room temperature, where allopurinol was used as a positive control. Each test compound was repeated three times. Enzyme activity determined in the absence of inhibitor was defined as 100%. The inhibition was calculated according to the following formula: inhibition (%) = [(reaction rate of control - reaction rate of sample)/ reaction rate of control] \times 100%.

2.3 Kinetic analysis for the inhibition of competitive type

To describe and study the inhibition mechanism of competitive type, the

Lineweaver–Burk (LB) equation can be expressed as:

$$\frac{1}{v} = \frac{K_m}{V_{\max}} \left(1 + \frac{[I]}{K_i} \right) \frac{1}{[S]} + \frac{1}{V_{\max}} \quad (1)$$

Secondary plots can be constructed from

$$K_m^{\text{app}} = \frac{K_m [I]}{V_{\max} K_i} + \frac{K_m}{V_{\max}}, \quad (2)$$

Where v , K_m and K_i represent the rate of the enzymatic reaction, the Michaelis–Menten constant and inhibition constant, respectively. The concentrations of inhibitors and substrates are expressed in terms of $[I]$ and $[S]$, respectively. The linear regression plot of $1/v$ vs. $1/[S]$ can be drawn to obtain the value of apparent Michaelis–Menten constant (K_m^{app}). If the secondary plot of K_m^{app} vs. $[I]$ is linearly fitted, suggesting that a single inhibition site or a single class of inhibition site[22].

2.4 Intrinsic fluorescence quenching

Spectrofluorometer FS5 (Edinburgh Instruments, England) equipped with a thermostat bath were employed to record the fluorescence emission spectra. Add a 2.0 mL solution containing 0.02 U/mL XO to a quartz cuvette, and then use a micropipette to continuously add 0.2 mmol/L TF1 solution for giving a concentration ranged from 0 to 57.14 $\mu\text{mol/L}$. The mixture was then put in the thermostatic bath for 5 minutes to reach equilibrium at various temperatures (288, 298 or 308 K). After excitation at 280 nm, fluorescence emission spectra were obtained at 290–500 nm. To correct the background fluorescence, the fluorescence of PBS was subtracted. In consideration of absorption of excitation light and re-absorption of emitted light, all data of the fluorescence obtained from these experiments were corrected by the following equation: [23]

$$F_c = F_m e^{(A_1 + A_2)/2} \quad (3)$$

The corrected and measured fluorescence are expressed in the terms of F_c and F_m , respectively. A_1 and A_2 are the absorbance of TF1 at excitation and emission wavelengths, respectively.

2.5 Molecular simulation

The probable interaction between TF1 and XO was further studied by using molecular docking technology (AutoDock, version 4.2.6). The 3D conformer of TF1 was downloaded from PubChem (<https://pubchem.ncbi.nlm.nih.gov/compound>), and the structure of XO (PDB ID: 1FIQ) was obtained from the RCSB PDB (<http://www.rcsb.org/pdb>)[3]. In order to perform the docking simulation, a grid box with dimensions of 90 Å×90 Å×120 Å was defined to make sure the whole active center enclosed. The grid maps with a grid spacing of 0.375 Å were calculated via using AutoGrid. Lamarckian genetic algorithm (LGA) was used for docking calculation, and the number of runs was set to 100 times. The docking conformation with the lowest binding energy among all clusters and/or in the largest cluster was selected for further analysis, which adopted the PyMOL molecular graphics system. LigPlot analysis is usually performed to understand the hydrophobic interaction between the ligand and enzyme[24], so the interaction between TF1 and XO was further analyzed via using software LigPlot⁺ (version 1.4.5).

2.6 Effects of TF1 on hyperuricaemia in mice

All animal experiments were performed according to the agreement of the Animal Protection and Use Committee of Putian University [NO. 2019(14)] and the ARRIVE

guidelines. Before the experiments, ICR mice (25-28g) were acclimated for at least 1 week. The method used to evaluate the effects of TF1 on animal hyperuricemic model was followed by the previous reported method with some adjustments[25]. There were five groups with six mice per group (n = 6) totally. Four groups, including the control, TF1 (100 mg/kg), TF1 (200 mg/kg) and allopurinol group, were injected intraperitoneally with potassium oxonate (PO) at a dosage of 250 mg/kg to raise the level of serum uric acid. Besides, a normal group was injected intraperitoneally with 1 ml 0.9% NaCl. After one hour, the mice in the TF1 (100 mg/kg) and TF1 (200 mg/kg) group were administrated TF1 intragastrically; in allopurinol group were administrated intragastrically in a dose of 20 mg/kg; in control group were administrated saline intragastrically. Two hours after PO induction, the whole blood samples of mice were collected. Blood was coagulated at room temperature for 1 hour, and then centrifuged at 3000 rpm for 5 mins to obtain serum. The level of serum uric acid was tested by the phosphotungstic acid method reported previously with some modifications[26].

2.7 Statistical analysis

The *in vitro* effects of TF1 on the activity of XO were evaluated three times (n = 3), while the animal studies included six mice in each group (n = 6). The results obtained were expressed as means \pm standard deviation (SD). To determine the significant difference at $p < 0.05$ or $p < 0.01$, one-way analysis of variance was performed by using EXCEL software (version 2007, Microsoft, USA) followed by multiple tests.

3 Results and discussion

3.1 Reversible inhibition effect of TF1 on XO

Fig. 1A shows the inhibitory effects of allopurinol (positive control) and TF1 on the activity of XO, indicating that both of them significantly inhibited the activity of XO with a positive correlation between the effects and dosages. Specifically, TF1 decreased the activity of XO to approximately 20% when its concentration reached to 166.67 $\mu\text{mol/L}$. Loss of 50% enzyme activity (IC_{50}) was occurred when the concentration of TF1 was $63.17 \pm 0.13 \mu\text{mol/L}$ (that of allopurinol was $4.43 \pm 0.06 \mu\text{mol/L}$), suggesting that TF1 was also an effective XO inhibitor. TF1 and its galloyl esters account for about 2% of the dried water extract of black tea, and they are proved to be safe by tea consumption over a long history worldwide[27]. Therefore, due to the serious side effects of allopurinol^[7], TF1 may be an alternative in the treatment of hyperuricaemia and gout.

As shown in Fig.1B, the curves of v vs. $[\text{XO}]$ were obtained at different concentrations of TF1, and proved that it mediated inhibition was reversible. The characteristic of good linearity is observed in the curves, all of which pass through the origin. In addition, with an increase of the concentration of TF1, the slope of the plots declines and it suggest that TF1 does not reduce the quantity of effective enzymes, but decrease the activity of all enzymes available. These results indicate that the inhibitory effect of TF1 on the activity of XO through non-covalent intermolecular interactions is reversible.

3.2 Inhibition kinetic of TF1 on the activity of XO

LB double reciprocal plots were employed to analyze the inhibitory type of TF1

against XO. As shown in Fig.1C, with the increase of TF1 concentration, the vertical axis intercept ($1/V_{max}$) of the LB plots remains unchanged, whereas the horizontal axis intercept ($-1/K_m$) increases; these results indicate that TF1 locates directly in the active center of XO as a typical competitive inhibitor to compete with the substrate (xanthine) in the catalytic process[28]. The secondary plot (Fig.1D) is linearly fitted, indicating only a single class of inhibition sites for TF1 against XO. The value of inhibition constant (K_i) was calculated to be $(9.96 \pm 0.94) \times 10^{-5}$ mol/L.

3.3 Effects of TF1 on the fluorescence of XO

Fluorescence quenching was used to further study the interaction between TF1 and XO. The fluorescence emission spectra of XO in the absence and presence of TF1 are shown in Fig.2A and 2B. Obviously, due to the tryptophan and tyrosine residues, XO exhibits a strong intrinsic fluorescence emission peak at 334 nm[29]. When the concentration of TF1 was increased, the fluorescence intensity of XO decreased dramatically with the emission peak unchanged, suggesting that TF1 interacted with XO and quenched its fluorescence.

In order to confirm the quenching mechanism of the combination of TF1 and XO, the data of fluorescence quenching had been further processed by the following equation (Stern-Volmer):

$$F_0/F = 1 + K_q\tau_0[Q] = 1 + K_{sv}[Q] \quad (4)$$

where F_0 and F are the fluorescence intensities before and after the addition of TF1, respectively. K_q , τ_0 , $[Q]$ and K_{sv} are the quenching rate constant of the biomolecule, the average lifetime of the fluorophore ($\tau_0=10^{-8}$ s), the concentration of TF1 and the

dynamic quenching constant of Stern–Volmer, respectively. As shown in Fig.2C, the plots of F_0/F vs. $[Q]$ all have excellent linearity within the studied concentrations, indicating that the formation of TF1–XO complex is a single quenching process by a manner of static or dynamic quenching. Then K_{sv} at 288, 298 and 308 K were obtained from the linear regress plots, the values of which were 7.69×10^4 , 5.73×10^4 and 4.25×10^4 L/mol, respectively, inversely correlating with temperature. Thus, it is easy to calculate the values of K_q , which were 7.69×10^{12} , 5.73×10^{12} and 4.25×10^{12} L/(mol·s) at 288, 298 and 308 K, respectively. It is obvious that they are much greater than the maximum scatter collision quenching constant [2.0×10^{10} L/(mol·s)][30]. Thus, it is safely to be inferred that static quenching plays a more significant role in the TF1–XO interaction[31], indicating the formation of a stable TF1–XO complex.

3.4 Number of Binding Sites of TF1 on XO

Given that it is a static quenching process, the apparent binding constant (K_a) and the number of binding sites (n) were obtained from a regression curve plotted according to the equation:

$$\log \frac{F_0 - F}{F} = \log K_a + n \log [Q] \quad (5)$$

The regression curve is presented in Fig.2D. The intercept and slope values of the curve were used to calculate K_a and n , which were 2.11×10^4 L/mol and 1.29 ($R = 0.996$) at 288 K, 2.00×10^4 L/mol and 1.23 ($R = 0.994$) at 298 K, and 1.64×10^4 L/mol and 1.22 ($R = 0.998$) at 308 K. The values of n for the TF1–XO complex are all equal to 1 independent with the temperatures, suggesting that there is a single class of TF1 binding sites on XO[32].

3.5 Thermodynamic analysis

The thermodynamic parameters (enthalpy change ΔH° and entropy change ΔS°) are very important, because they can help to elucidate the major forces in the formation of TF1–XO complex. If there is no significant change in temperature, the value of ΔH° and ΔS° can be considered as a constant and determined by the van't Hoff equation below:

$$\log K_a = -\frac{\Delta H^\circ}{2.303RT} + \frac{\Delta S^\circ}{2.303R} \quad (6)$$

Where K_a is the binding constant at the corresponding temperature (288, 298 and 308 K); T and R represent the experimental temperature (K) and the universal gas constant [8.314 J/(mol·K)], respectively. Then the value of ΔG° (free energy change) can be calculated via using the equation below:

$$\Delta G^\circ = \Delta H^\circ - T\Delta S^\circ \quad (7)$$

The calculated thermodynamic parameters are listed in Table 1. According to the negative values of ΔG° and ΔH° , a spontaneous and exothermic process between TF1 and XO is proposed. Moreover, the positive value of ΔS° and the negative value of ΔH° indicated that there are mainly hydrophobic effects and hydrogen bonds between TF1 and XO[33, 34].

3.6 Computational docking analysis

A re-docked method with some modifications was employed to validate the docking procedure[6]. In brief, the original ligand salicylic acid was re-docked into XO using the procedure described in the section 2.5. The results showed that the docked conformation of salicylic acid was similar with the original X-ray structure[3],

suggesting that docking procedure is corroborated. And then, molecular docking study was performed to further understand the binding mode of the complexes formed between TF1 and XO. According to the cluster analysis, the conformation with the lowest binding energy (-7.81 kcal/mol) in all the clusters was considered to be the optimal conformation, while the conformation with the lowest binding energy (-7.18 kcal/mol) in the biggest cluster was considered as the suboptimal conformation. The binding energy of TF1 conformations are almost equal to that of the substrate xanthine (-7.1 kcal/mol)[35], suggesting that TF1 may have roughly the same binding affinity as xanthine with XO, which may be the reason why the inhibitory effects of TF1 on XO is relatively low. Moreover, the binding energy of either the optimal or suboptimal conformation is slightly lower than ΔG° (-5.83 kcal/mol, equal to -24.41 kJ/mol listed in table 1). Although the calculated value is slightly different from the experimental value, it shows that the interaction between TF1 and XO is spontaneous. As presented in Fig. 3A and 3C, both the optimal and suboptimal conformations of TF1 appear in the active cavity (marked in color) of XO. The active center, mainly composed of various residues such as Leu-648, Asn-768, Glu-802, Ser-876, Glu-879, Arg-880, Phe-914, Phe-1009, Thr-1010, Val-1011, Leu-1014 and Pro-1076, is a long narrow path, through which the substrate may reach the catalytic site easily (Mo-pt cofactor)[36, 37]. When an inhibitor TF1 located in the active cavity, the path was mostly blocked. Thus it may prevent the substrate (xanthine) from entering the catalytic site and ultimately hindering its oxidation[36]. As for the optimal conformation (Fig.3B), TF1 is located in the active cavity by forming 5 hydrogen

bonds with residues Leu-648 ($d=2.0$ Å), Asn-768 ($d=2.0$ Å), Glu-802 ($d=2.0$ Å), Glu-879 ($d=1.8$ Å) and Thr-1010 ($d=1.9$ Å), which are believed to form the active cavity[36]. The suboptimal conformation (Fig.3D) also binds with XO via forming 6 hydrogen bonds with amino acid residues Asn-768 ($d=1.7$ Å and 2.5 Å), Lys-771 ($d=2.1$ Å and 2.6 Å) and Glu-802 ($d=1.7$ Å and 2.2 Å), some of which also take part in forming the active cavity[36]. These findings indicate that hydrogen bonding plays a key role in the binding of TF1 to XO. In addition, it has been proved that Glu-802 plays an important role in the hydroxylation of xanthine[38], suggesting that both the optimal and suboptimal conformations have the similar binding region as the substrate. The second interaction force between TF1 and XO was from hydrophobic interactions[39], which were analyzed by LigPlot⁺. The results (Fig.3E) show the hydrophobic interactions between the optimal conformation of TF1 and the 12 residues of XO, including Glu-879, Pro-1012, Thr-1010, Val-1011, Lys-771, Glu-802, Pro-1076, Leu-873, Leu-1014, Asn-768, Leu-648 and Phe-649. As shown in Fig.3F, the suboptimal conformation of TF1 is surrounded by 14 residues of XO, including Asn-768, Leu-1014, Ser-1075, Pro-1076, Met-770, Lys-771, Phe-649, Phe-1013, Val-1011, His-875, Ser-876, Leu-648, Leu-873 and Glu-802. Most of these residues, such as Glu-802, Thr-1010, Leu-873, Val-1011 and Leu-648, were described as catalytic residues[40], and the others were all distributed around the Mo-pt center. All these hydrophobic interactions help TF1 to hold in the binding site of the XO. The docking results suggest that TF1 binds to XO through hydrogen bonds and hydrophobic interactions, producing a steric impediment to the entry of the substrate

into the active site.

3.7 The anti-hyperuricaemia effect of TF1 in mice

Given that the inhibitory effects of TF1 on XO, the anti-hyperuricaemia effect of TF1 in mice was further investigated. Mouse model of hyperuricaemia was induced by intraperitoneal injection of potassium oxonate (PO, an uricase inhibitor). The results presented in Fig.4 show that the normal serum uric acid level in mice is 2.39 mg/dL. After injection of PO for 2 hours, the level of uric acid in control group reaches to 5.59 mg/dL, which is significantly higher than the normal group. After intragastric administration of TF1 (100 mg/kg) in hyperuricemic mice, the value of serum uric acid drops to 5.17 mg/dL, but there is no significant difference when it compared with the control. When the dosage reaches to 200 mg/kg in hyperuricemic mice, the value of serum uric acid drops to 3.61 mg/dL, which shows a significant decrease compared to the control group. After intragastric administration of allopurinol (20 mg/kg), the serum uric acid of mice drops significantly to 2.59 mg/dl. The results suggest that TF1 indeed has anti-hyperuricaemia effect, but its effect is lower than that of allopurinol. This may be due to the different inhibitory effects of TF1 and allopurinol on XO, which has been confirmed in section 2.2 of this study. However, due to the confirmed long-term safety of TF1, it may have potential clinical applications in the treatment of gout and other metabolic disorders.

4. Conclusions

The inhibitory mechanism of TF1 on XO and its anti-hyperuricaemia effect in mice have been investigated in this study. In summary, the key findings of our study are as

follows: (i) TF1 inhibited the activity of XO in a reversible and competitive manner with an IC_{50} value of $63.17 \pm 0.13 \mu\text{mol/L}$ and K_i value of $(9.96 \pm 0.94) \times 10^{-5} \text{ mol/L}$; (ii) a static and strong fluorescence quenching of XO occurred because of the formation of TF1-XO complexes; (iii) thermodynamic analysis showed that the formation of TF1-XO complexes was a spontaneous process mainly driven by hydrogen bonds and hydrophobic interactions; (iv) molecular simulation suggested that TF1 located in the catalytic center via interacting with some residues, such as Glu-879, Pro-1012, Thr-1010, Val-1011, Lys-771, Glu-802, Pro-1076, Leu-873, Leu-1014, Asn-768, Leu-648 and Phe-649; and (v) the results of animal experiments suggested that TF1 exhibited anti-hyperuricaemia effect in hyperuricemic mice. As a consequence, the possible reason for the inhibition of XO activity is the insertion of TF1 into the active center of XO, thus hindering the entry of xanthine. We propose a novel inhibition mechanism that provides new insights into the interaction between TF1 and XO and confirm the anti-hyperuricaemia effect in mice, indicating that TF1 can be a promising XO inhibitor for the treatment of hyperuricaemia and other related metabolic diseases.

CRediT author statement

Jianmin Chen: Conceptualization, Methodology, Writing- Original draft preparation;
Qinglian Li: Software, Investigation; **Yaling Ye:** Investigation, Data curation;
Mengnan Ran: Supervision, Data curation; **Zhipeng Ruan:** Supervision, Validation;
Nan Jin: Reviewing and Editing.

Conflict of interest

We declare that we do not have any commercial or associative interest that represents a conflict of interest in connection with the work submitted.

Acknowledgements

This work was supported by the Natural Science Foundation of Fujian Province (Grant No.2019J01806), the Putian Science and Technology Bureau (Grant No. 2018SP3004) and Training Program of Innovation and Entrepreneurship for Undergraduates (Grant No. 201911498055, 201811498003 and 201811498027).

References

- [1] F. Borges, E. Fernandes, F. Progress towards the discovery of xanthine oxidase inhibitors, *Current Medicinal Chemistry* 9(2) (2002) 195-217.
- [2] T.P. Dew, A.J. Day, M.R.A. Morgan, Xanthine oxidase activity in vitro: effects of food extracts and components, *Journal of Agricultural & Food Chemistry* 53(16) (2005) 6510-5.
- [3] C. Enroth, B.T. Eger, K. Okamoto, T. Nishino, E.F. Pai, Crystal structures of bovine milk xanthine dehydrogenase and xanthine oxidase: structure-based mechanism of conversion, *Proceedings of the National Academy of Sciences of the United States of America* 97(20) (2000) 10723-10728.
- [4] F. Candan, EFFECT OF RHUS CORIARIA L. (ANACARDIACEAE) ON SUPEROXIDE RADICAL SCAVENGING AND XANTHINE OXIDASE ACTIVITY, *J Enzyme Inhib Med Chem* 18(1) (2003) 59-62.
- [5] D. Yi, H. Huang, M. Zhao, D. Sun-Waterhouse, L. Lin, C. Xiao, Mechanisms underlying the xanthine oxidase inhibitory effects of dietary flavonoids galangin and pinobanksin, *Journal of Functional Foods* 24 (2016) 26-36.
- [6] M. Rezaeinasab, A. Benvidi, S. Gharaghani, S. Abbasi, H.R. Zare, Electrochemical investigation of the inhibition effect of carvacrol on xanthine oxidase activity merging with theoretical studies, *Process Biochemistry* 83 (2019) 86-95.
- [7] P. Pacher, A. Nivorozhkin, C. Szabo, Therapeutic effects of xanthine oxidase inhibitors: renaissance half a century after the discovery of allopurinol, *Pharmacol Rev* 58(1) (2006) 87-114.
- [8] M. Rezaeinasab, A. Benvidi, S. Gharaghani, S. Abbasi, H.R. Zare, Deciphering the inhibition effect of thymoquinone on xanthine oxidase activity using differential pulse voltammetry in combination with theoretical studies, *Enzyme and Microbial Technology* 121 (2019) 29-36.
- [9] B. Mathew, J. Suresh, G. E. Mathew, S. A. Rasheed, J. K. Vilapurathu, P. Jayaraj, Flavonoids: An Outstanding Structural Core for the Inhibition of Xanthine Oxidase Enzyme, *Current Enzyme Inhibition*

11(2) (2015) 108-115.

- [10] G. Ying, G.O. Rankin, T.U. Youying, Y.I. CHARLIE CHEN, Inhibitory Effects of the Four Main Theaflavin Derivatives Found in Black Tea on Ovarian Cancer Cells, *Anticancer Research* 36(2) (2016) 643-651.
- [11] J. Zhang, S. Cai, J. Li, L. Xiong, L. Tian, J. Liu, J. Huang, Z. Liu, Neuroprotective Effects of Theaflavins Against Oxidative Stress-Induced Apoptosis in PC12 Cells, *Neurochemical Research* 41(12) (2016) 3364-3372.
- [12] L. Leung, Y. Su, R. Chen, Z. Zhang, Y. Huang, Z. Chen, Theaflavins in black tea and catechins in green tea are equally effective antioxidants, *Journal of Nutrition* 131(9) (2001) 2248-2251.
- [13] A. Cantatore, S.D. Randall, D. Traum, S.D. Adams, Effect of black tea extract on herpes simplex virus-1 infection of cultured cells, *Bmc Complementary & Alternative Medicine* 13(1) (2013) 139.
- [14] D. Jin, X. Yi, M. Xin, Q. Meng, G. Ying, L. Bo, Y. Tu, Antiobesity and lipid lowering effects of theaflavins on high-fat diet induced obese rats, *Journal of Functional Foods* 5(3) (2013) 1142-1150.
- [15] A.J. Kobalka, R.W. Keck, J. Jankun, Synergistic anticancer activity of biologicals from green and black tea on DU 145 human prostate cancer cells, 40(401) (2015) 1-4.
- [16] M. Zu, F. Yang, W. Zhou, A. Liu, G. Du, L. Zheng, In vitro anti-influenza virus and anti-inflammatory activities of theaflavin derivatives, *Antiviral Res* 94(3) (2012) 217-224.
- [17] M.P.P. Stanely, N.K. Kannan, Protective effect of rutin on lipids, lipoproteins, lipid metabolizing enzymes and glycoproteins in streptozotocin-induced diabetic rats, *Journal of Pharmacy & Pharmacology* 58(10) (2010) 1373-1383.
- [18] K. Nishikawa, Y. Iwamoto, Y. Kobayashi, F. Katsuoka, S.-i. Kawaguchi, T. Tsujita, T. Nakamura, S. Kato, M. Yamamoto, H. Takayanagi, M. Ishii, DNA methyltransferase 3a regulates osteoclast differentiation by coupling to an S-adenosylmethionine-producing metabolic pathway, *Nature Medicine* 21(3) (2015) 281-287.
- [19] J.K. Lin, P.C. Chen, C.T. Ho, S.Y. Lin-Shiau, Inhibition of xanthine oxidase and suppression of intracellular reactive oxygen species in HL-60 cells by theaflavin-3,3'-digallate, (-)-epigallocatechin-3-gallate, and propyl gallate, *Journal of Agricultural & Food Chemistry* 48(7) (2000) 2736.
- [20] C. Zhu, L.-L. Tai, X.-c. Wan, D.-x. Li, Y.-Q. Zhao, Y. Xu, Comparative effects of green and black tea extracts on lowering serum uric acid in hyperuricemic mice, *Pharmaceutical Biology* 55(1) (2017) 2123-2128.
- [21] W. Nan, Z. Yuangang, F. Yujie, K. Yu, Z. Jintong, L. Xiaojuan, L. Ji, W. Michael, E. Thomas, Antioxidant activities and xanthine oxidase inhibitory effects of extracts and main polyphenolic compounds obtained from *Geranium sibiricum* L, *J Agric Food Chem* 58(8) (2010) 4737-4743.
- [22] Y.-X. Si, Z.-J. Wang, D. Park, H.Y. Chung, S.-F. Wang, L. Yan, J.-M. Yang, G.-Y. Qian, S.-J. Yin, Y.-D. Park, Effect of hesperetin on tyrosinase: Inhibition kinetics integrated computational simulation study, *International Journal of Biological Macromolecules* 50(1) (2012) 257-262.
- [23] Y. Wang, G. Zhang, J. Pan, D. Gong, Novel insights into the inhibitory mechanism of kaempferol on xanthine oxidase, *Journal of Agricultural & Food Chemistry* 63(2) (2015) 526-34.
- [24] A.C. Wallace, R.A. Laskowski, J.M. Thornton, LIGPLOT: a program to generate schematic diagrams of protein-ligand interactions, *Protein Engineering* 8(2) (1995) 127-134.
- [25] S.Y. Wang, C.W. Yang, J.W. Liao, W.W. Zhen, F.H. Chu, S.T. Chang, Essential oil from leaves of *Cinnamomum osmophloeum* acts as a xanthine oxidase inhibitor and reduces the serum uric acid levels in oxonate-induced mice, 15(11) (2008) 940-945.

- [26] J.J. Carroll, H. Coburn, R. Douglass, A.L. Babson, A Simplified Alkaline Phosphotungstate Assay for Uric Acid in Serum, *Clinical Chemistry* 17(3) (1971) 158-160.
- [27] S. Liu, H. Lu, Q. Zhao, Y. He, J. Niu, A.K. Debnath, S. Wu, S. Jiang, Theaflavin derivatives in black tea and catechin derivatives in green tea inhibit HIV-1 entry by targeting gp41, *Biochimica et Biophysica Acta (BBA) - General Subjects* 1723(1) (2005) 270-281.
- [28] Y. Wang, G. Zhang, J. Pan, D. Gong, Novel Insights into the Inhibitory Mechanism of Kaempferol on Xanthine Oxidase, *Journal of Agricultural & Food Chemistry* 63(2) (2015) 526-534.
- [29] J. Yan, G. Zhang, Y. Hu, Y. Ma, Effect of luteolin on xanthine oxidase: Inhibition kinetics and interaction mechanism merging with docking simulation, *Food Chemistry* 141(4) (2013) 3766-3773.
- [30] O.K. Abou-Zied, O.I. Al-Shihi, Characterization of subdomain IIA binding site of human serum albumin in its native, unfolded, and refolded states using small molecular probes, *J. Am. Chem. Soc.* 130(32) (2008) 10793-10801.
- [31] Y. Wang, G. Zhang, J. Yan, D. Gong, Inhibitory effect of morin on tyrosinase: insights from spectroscopic and molecular docking studies, *Food Chem.* 163 (2014) 226-233.
- [32] S. Shaikh, J. Seetharamappa, P. Kandagal, S. Ashoka, Binding of the bioactive component isothipendyl hydrochloride with bovine serum albumin, *J. Mol. Struct.* 786(1) (2006) 46-52.
- [33] C. Tang, L. Zhu, Y. Chen, R. Qin, Z.N. Mei, J. Xu, G. Yang, Synthesis and biological evaluation of oleanolic acid derivative-chalcone conjugates as α -glucosidase inhibitors, *Rsc Advances* 4(21) (2014) 10862-10874.
- [34] P.D. Ross, S. Subramanian, Thermodynamics of protein association reactions: forces contributing to stability, *Biochemistry* 20(11) (1981) 3096-3102.
- [35] S. Honda, Y. Fukuyama, H. Nishiwaki, A. Masuda, T. Masuda, Conversion to purpurogallin, a key step in the mechanism of the potent xanthine oxidase inhibitory activity of pyrogallol, *Free Radical Biology and Medicine* 106 (2017) 228-235.
- [36] S. Lin, G. Zhang, Y. Liao, J. Pan, Inhibition of chrysin on xanthine oxidase activity and its inhibition mechanism, *International Journal of Biological Macromolecules* 81 (2015) 274-282.
- [37] P. Jayaraj, B. Mathew, B. Parimaladevi, V.A. Ramani, R. Govindarajan, Isolation of a bioactive flavonoid from *Spilanthes calva* D.C. in vitro xanthine oxidase assay and in silico study, *Biomedicine & Preventive Nutrition* 4(4) (2014) 481-484.
- [38] T. Nishino, K. Okamoto, B.T. Eger, E.F. Pai, T. Nishino, Mammalian xanthine oxidoreductase – mechanism of transition from xanthine dehydrogenase to xanthine oxidase, *The FEBS Journal* 275(13) (2008) 3278-3289.
- [39] E. Hofmann, J. Webster, T. Do, R. Kline, S. Paula, Hydroxylated chalcones with dual properties: Xanthine oxidase inhibitors and radical scavengers, *Bioorganic & Medicinal Chemistry* 24(4) (2015) 578-587.
- [40] H. Cao, J.M. Pauff, R. Hille, X-ray Crystal Structure of a Xanthine Oxidase Complex with the Flavonoid Inhibitor Quercetin, *Journal of Natural Products* 77(7) (2014) 1693-1699.

Figure Legends

Fig.1. (A) Inhibitory effects of allopurinol and theaflavin (TF1) on the activity of xanthine oxidase (XO) (pH 7.4, T = 298 K). The structures of allopurinol and TF1 are presented in the inset. The concentrations of xanthine and XO used in these experiments were 1.0×10^{-4} mol/L and 0.04 U/mL, respectively. (B) Plots of v vs. [XO]. $c(\text{xanthine}) = 1.0 \times 10^{-4}$ mol/L, and $c(\text{TF1}) = 0, 20.83, 41.67, 83.33$ and 166.67 $\mu\text{mol/L}$ for curves a→e, respectively. (C) LB plots. $c(\text{XO}) = 0.04$ U/mL, and $c(\text{TF1}) = 0, 20.83, 41.67, 83.33$ and 166.67 $\mu\text{mol/L}$ for curve a→e, respectively. (D) The secondary plot of K_m^{app} (slope) vs. [TF1].

Fig.2. (A) Intrinsic fluorescence emission spectra of xanthine oxidase (XO) under the existence of theaflavin (TF1) with different concentrations, which were 0, 9.52, 18.18, 26.08, 33.33, 40.00, 46.15, 51.85 and 57.14 $\mu\text{mol/L}$ for curves (a–i), respectively. (B) Relative fluorescence intensity (%) of XO in the presence of TF1 with different concentrations (298K). (C) The plots based on Stern–Volmer equation for studying the quenching effects of TF1 on the intrinsic fluorescence of XO at different temperatures (288, 298 and 308 K). (D) Secondary plots of $\log [(F_0-F)/F]$ vs. $\log [Q]$ at different temperatures (288, 298 and 308 K).

Fig.3. Molecular docking of the interactions between theaflavin (TF1) and xanthine oxidase (XO): (A) the magenta sphere represent Mo ions, which is surrounded by various residues (marked in color) to develop the active cavity; the coarser stick in

cyan represents for TF1 lies in the active cavity. (B) Details between TF1 (the optimal conformation) and XO, the dashed line in yellow represents hydrogen-bond. (C) The suboptimal conformation lies in the active cavity. (D) Details between TF1 (the suboptimal conformation) and XO. (E, F) Hydrophobic interactions between TF1 [the optimal (E) and suboptimal conformation (F)] and XO.

Fig.4. Dose-dependent anti-hyperuricaemia effects of theaflavin (TF1) and allopurinol in mice. Normal: mice without treatment; Control: mice treated with potassium oxonate (PO); Allopurinol: mice treated with PO followed by administering 20 mg/kg allopurinol intragastrically; TF1 (100 mg/kg): mice treated with PO followed by administering 100 mg/kg TF1 intragastrically; TF1 (200 mg/kg): mice treated with PO followed by administering 200 mg/kg TF1 intragastrically. The data were presented as mean \pm SD. *P0.05, **P0.01 when the drug treated group was compared with the hyperuricemic control group.

Table 1 Kinetic and thermodynamic parameters of the interaction between theaflavin (TF1) and xanthine oxidase (XO) under different temperatures.

T(K)	$K_{sv}(\times 10^4 \text{L/mol})$	R^a	$K_a(\times 10^4 \text{L/mol})$	R^b	n	$\Delta H^\circ(\text{kJ/mol})$	$\Delta G^\circ(\text{kJ/mol})$	$\Delta S^\circ[\text{J}/(\text{mol}\cdot\text{K})]$
288	7.688±0.04	0.9905	2.11±0.02	0.9959	1.291±0.03	-9.28±0.16	-23.91±0.24	50.79±0.12
298	5.730±0.03	0.9857	2.00±0.02	0.9941	1.231±0.03		-24.41±0.22	
308	4.246±0.03	0.9931	1.64±0.01	0.9986	1.215±0.02		-24.92±0.31	

R^a and R^b represent the correlation coefficient for the K_{sv} and K_a values, respectively.

Figures

Fig.1

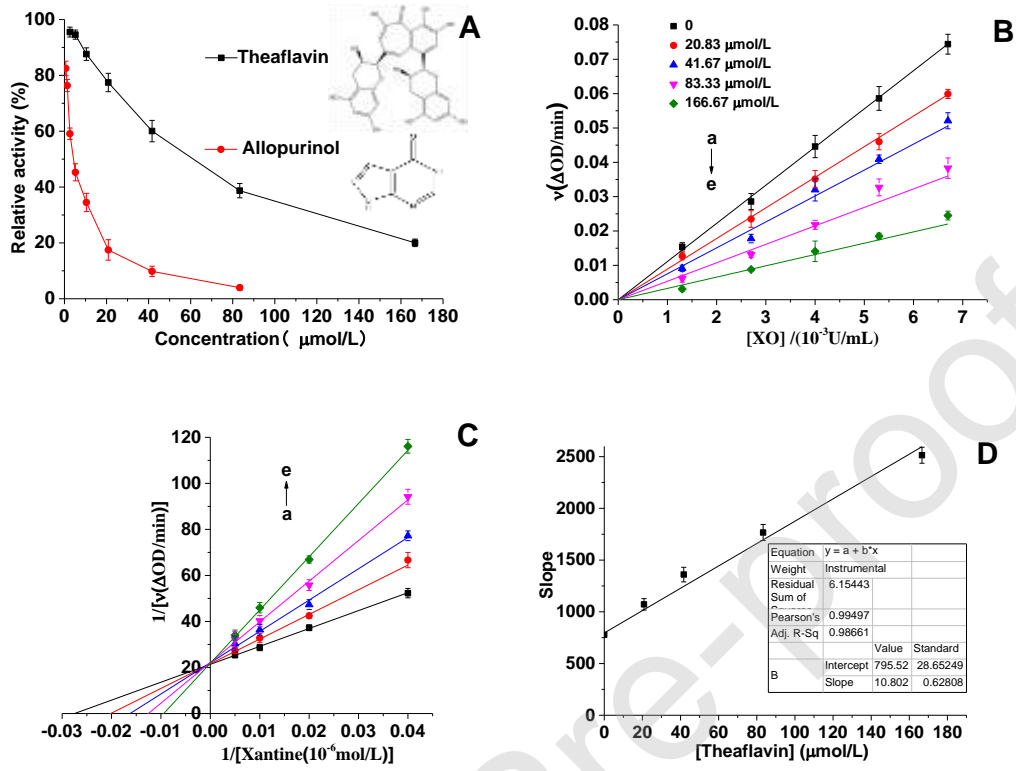


Fig.2

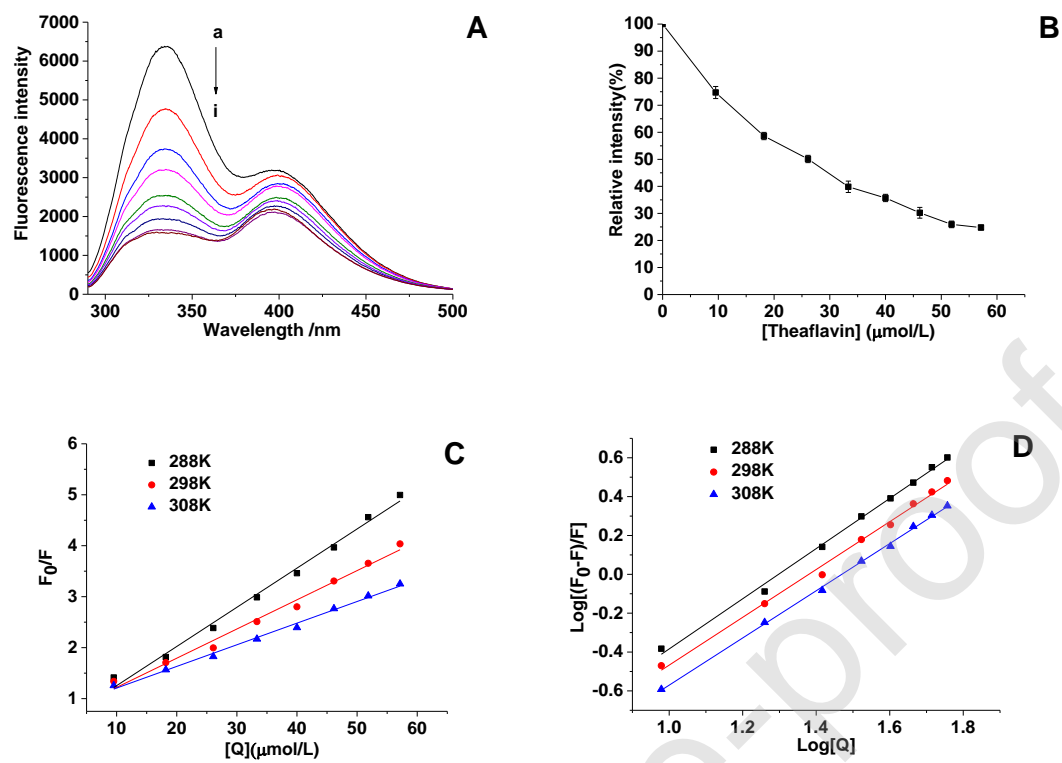


Fig.3

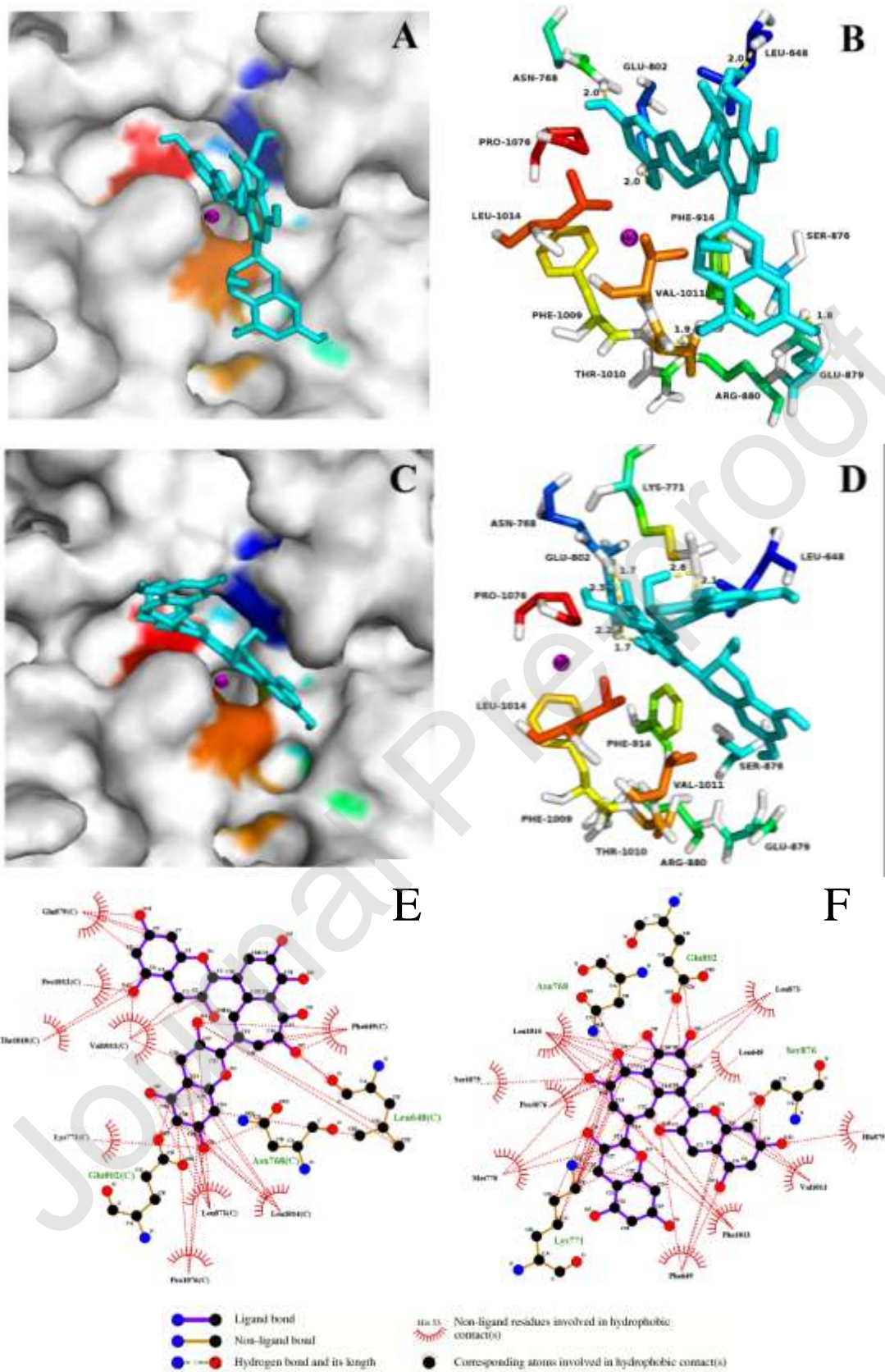


Fig.4

